

# A Laser-Plasma Ion Beam Booster Based on Hollow-Channel Magnetic Vortex Acceleration

Marco Garten, Stepan S. Bulanov, Sahel Hakimi, Lieselotte Obst-Huebl, Chad E. Mitchell,  
Carl Schroeder, Eric Esarey, Cameron G. R. Geddes, Jean-Luc Vay, and Axel Huebl\*

*Lawrence Berkeley National Laboratory  
1 Cyclotron Rd, Berkeley (CA), 94720, USA*

(Dated: August 10, 2023)

Laser-driven ion acceleration can provide ultra-short, high-charge, low-emittance beams. Although undergoing extensive research, demonstrated maximum energies for laser-ion sources are non-relativistic, complicating injection into high- $\beta$  accelerator elements and stopping short of desirable energies for pivotal applications, such as proton tumor therapy. In this work, we decouple the efforts towards relativistic beam energies from a single laser-plasma source via a proof-of-principle concept, boosting the beam into this regime through only a few plasma stages. We employ full 3D particle-in-cell simulations to demonstrate the capability for capture of high-charge beams as produced by laser-driven sources, where both source and booster stages utilize readily available laser pulse parameters.

Plasma-based accelerators have been intensely studied over the past decades to harness their many promising features. Field strengths in a plasma are between a hundred to a million times higher than in conventional machines. This allows for particle beam sources of very high-charge ( $\gg 100$  pC) and intensity, often shorter than the driving laser pulse length (e.g.,  $\leq 30$  fs), and more compact accelerator footprints. Most prominently, plasma-wakefield accelerators are a candidate for next generation electron-positron colliders for high-energy physics and light sources [1]. However, plasma-ion acceleration to high ion energies turns out to be significantly more challenging, even at modern Petawatt laser facilities [2, 3] able to deliver high-intensity laser pulses reaching  $10^{23}$  W/cm<sup>2</sup> [4]. Due to significantly lower charge-to-mass ratio than that of electrons or positrons, ions require much stronger and more spatially localized electric fields to be efficiently accelerated. Depending on the laser intensity, target density, thickness, and composition, a specific laser-ion acceleration mechanism might dominate [5–7]. Usually, target normal sheath acceleration (TNSA), Coulomb explosion (CE), radiation pressure acceleration (RPA), and magnetic vortex acceleration (MVA) are identified as the basic regimes [8, 9], each corresponding to a set of laser-target interaction parameters.

The demonstrated highest cut-off ion energies are of the range of 60–100 MeV for protons [10–12], which is only a factor 2–3 short of the needs of medical applications such as proton tumor therapy [13–15]. Many laser-ion acceleration mechanisms [8] offer a favorable scaling of maximum ion energies with laser power. Yet, advancing system laser power is a multi-decade long undertaking and often significantly reduces laser repetition rate, temporal laser contrast that impedes the acceleration, and increases facility cost and footprint [2, 3]. Since

it is furthermore desirable to reach relativistic ion energies, e.g., for specific applications or for injection into a plasma-based accelerator that requires initially relativistic (high- $\beta$ ,  $\beta = v/c$  is the normalized ion velocity) particle energies [16–18], a different approach to laser ion acceleration is needed. Thus, we propose to employ an approach tested in laser plasma acceleration of electrons, namely, staged acceleration [19]. In contrast to staged electron acceleration, where a single laser-plasma stage readily provides relativistic particles, the one for ions should be achieved by first employing quasi-static fields to boost ion energy from non-relativistic to relativistic values. Here we explore the laser-target setup typical for MVA as booster stages. Realizing MVA involves the interaction of an intense laser pulse with an optically opaque plasma target, near the critical plasma density  $n_c$ , of several tens of micrometer thickness [20–22]. The ponderomotive force of the laser pulse generates a plasma channel, first in electron density, then in ion density, and propagates inside this self-generated channel. During this propagation, the laser generates a strong electron current in the forward direction, which, at some point, starts to pinch, creating an electron and ion filament along the laser propagation axis. As the laser, electrons and ions exit the target from the back side, strong electric and magnetic fields are generated there, producing a high-flux ion beam of ultra-short time structure and with nano-Coulombs of charge [23, 24].

For MVA, the electric fields created at the rear side of the plasma channel are not only accelerating for ions, but also focusing in nature. Quasi-static magnetic fields arising from the interplay of a forward-accelerated electron filament and cold return currents in the channel walls generate these fields [23, 24]. MVA has been approached in multiple experiments [9, 25–30], and was found to be robust against laser contrast and incidence angle variations in extensive numerical modeling studies [31]. The near-critical density of MVA targets relaxes the requirements for microscopic fabrication precision needed for exploiting other mechanisms. Near-critical density targets

---

\* axelhuebl@lbl.gov

also optimize laser energy absorption. Still, accelerating fields reach tens of TV/m strengths. Particularly attractive for energy boosting is that upon laser irradiation no potential barrier is created at the target front-side [32–35]. Therefore, particles do not experience strong deceleration before entering the MVA channel. Moreover, laser-driven ion sources were shown to deliver very laminar, ultra-low emittance beams [36–38]. Thus, it is plausible to expect that these beams can be coupled to booster stages.

Existing work on boosting the energy of laser-driven ion beams can be classified into different categories: First, energy boosting in cascades of acceleration mechanisms, using a single laser pulse and composite target [39–42] or multiple targets [18]. Second, energy can be boosted using multiple laser pulses on a single target [43–45]. Both approaches are limited by the available laser energy. Third, proposing to overcome this limitation, energy boosting with multiple laser pulses and staged targets [32, 34, 46, 47], so far with limited exploration of performance with intense beams or preservation of important beam moments, besides gaining energy.

This letter studies MVA as a scalable mechanism for boosting an ultra-intense, high-charge beam that is implementable with high-repetition rate stages [9, 48, 49]. We investigate and propose a robust scheme in which accepted ion beam velocities can vary significantly for each booster stage and systematically evaluate temporal and position tolerances. Critical for staging into subsequent high- $\beta$  acceleration stages, our approach can conserve the intense charge and control the ultra-low emittance of laser-plasma generated beams. Transport between plasma booster stages can be achieved via a hybrid beamline: Plasma ion boosters would be connected with conventional beam-shaping and transport elements to ensure that the right phase space conditions for acceptance into the booster can be configured.

In this paper, a booster stage based on the high-intensity laser pulse interaction with a near critical density (NCD) target (an MVA-type setup) is studied. However, there is an important distinction between a typical MVA target and the one proposed here. In MVA, the accelerated ions originate from a central filament, which is formed from the background ions under the action of the pinched electron current. Those ions mainly come from the back of the target from a small region near the channel axis. Thus, in order to suppress the MVA from the booster stage itself, an NCD target with a pre-made hollow region is chosen. Hollow targets are actively pursued for laser-plasma acceleration of electrons, positrons, and ions (see, e.g., [50–53]) and can be generated with micromachining or additional laser pulses [54–56].

Typically, MVA relies on the intense laser pulse self-channeling in an NCD plasma [23, 24, 57]. The balance of the ponderomotive push by the laser and the Coulomb attraction between the displaced electrons and remaining ions determine the radius of such a channel. In the case of an NCD plasma with a pre-made hole of radius  $r_h$  the

radius of the channel  $R_{ch}$  and the amplitude of the laser field  $a_{ch}$  in the channel can be determined using the same line of reasoning:

$$\frac{\pi^2}{\lambda^2} (R_{ch}^2 - r_h^2) = a_{ch}(r_h) \frac{n_{cr}}{n_e}, \quad (1)$$

$$\frac{\pi^2 R_{ch}^2}{\lambda^2} a_{ch}^2 = \frac{2P}{KP_c}. \quad (2)$$

Here  $a_{ch}(r_h) = a_{ch} [J_0(\kappa r_h) - J_2(\kappa r_h)]$ , which comes from the solution of the wave equation in the wave guide [23],  $J_0$  and  $J_2$  are the Bessel functions, and  $\kappa = 1.84/R_{ch}$ .  $P_c = 2m_e^2 c^5 / e^2 = 17$  GW is a characteristic power for relativistic self-focusing,  $n_{cr} = m_e \omega^2 / (4\pi e^2)$  is the plasma critical density,  $\lambda$ ,  $\omega$ , and  $P$  are the laser wavelength, frequency, and power respectively,  $e$  and  $m_e$  are electron charge and mass, and  $K = 1/13.5$  is a geometric factor. In the case  $r_h = 0$ , these two equations reduce to the results of Ref. [57]. For the parameters used below the radius of the channel is  $R_{ch} = 2.1 \mu\text{m}$ , which is only 5% smaller than in the case of a homogeneous NCD plasma.

As it was mentioned above, the accelerating and focusing fields at the back of the target are due to the strong electron current flowing through the channel in the wake of the laser pulse. The peak value of the magnetic field generated by such a current scales as  $B_{ch} \sim n_e R_{ch}^3$ . Thus, the main difference in field strength between the targets with and without hole is caused by different amount of electrons available in the channel, which can be accounted for by the factor  $(1 - r_h^2/R_{ch}^2)$ .

To study our approach, we performed 3D3V particle-in-cell simulations with the code WarpX [58, 59], using parameters readily available at existing PW laser facilities like the newly commissioned BELLA iP2 beamline [60]. The laser pulse has a normalized amplitude of  $a_0 = 42$ , a central wavelength of 815 nm, a duration of 29.8 fs, and a beam waist of 2.12  $\mu\text{m}$ .

Every presented booster stage length is 28  $\mu\text{m}$ , density is  $2n_c$  and hole radius is  $r_{hole} = 1.5 \mu\text{m}$ . Since the incoming ion beam is non-relativistic for early stages, it is entering the plasma stage before the laser pulse, which during the course of the propagation overtakes the ion beam. A hollow channel reduces the ion beam interaction with plasma on the axis of the stage, while the laser pulse waist is larger to drive a strong channel current at radius  $R_{ch}$  for acceleration at the stage rear. The laser-target interaction pulls electrons off the channel wall and creates an electron filament on the channel axis, as in regular MVA (see Fig. 1). When the pulse and the filament pass the target rear, MVA-typical accelerating and focusing fields are created. The ion beam is temporally phase matched to arrive where and when the fields are strongest. It experiences the optimum acceleration before the electron filament disperses again and field strengths subside. In simulations, no degradation of beam quality was found from direct laser-beam interaction and acceleration occurs at the target rear.

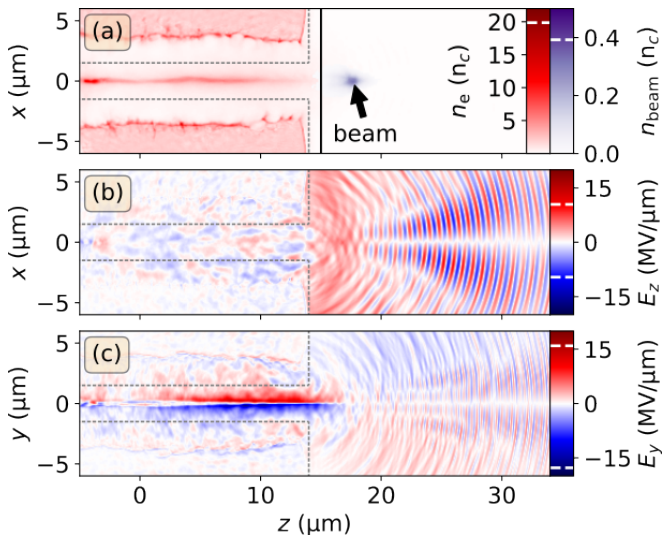


FIG. 1. *Fields of the booster stage with a 200 pC proton beam.* The stage center is at  $z = 0 \mu\text{m}$ . (a) Electron density  $n_e$  in red, reference plane at the beam focus  $z^* = 15 \mu\text{m}$  (black vertical line), and beam density  $n_{\text{beam}}$  in purple located behind the exit of the stage. (b) Accelerating electric field  $E_z$ , and (c) focusing electric field  $E_y$  shown 283 fs after simulation start. White dashed lines inside the colorbars denote current maximum and minimum values, respectively. Dashed grey lines mark the outline of the initial electron density of the hollow channel.

To characterize the proton beams that can be energy-boostered in a Petawatt-laser driven, hollow MVA stage, the longitudinal and transverse acceptance of protons are measured by recording the energy gain after the booster stage from particles with varying initial momenta and time delays with respect to the laser pulse arriving at a reference plane. In Figure 1, the plane of reference is at  $z^* = 15 \mu\text{m}$ .

Figure 2 shows the longitudinal beam acceptance, a measure for accepted beam length and temporal jitter between beam and laser pulse. For the energy gain, particles were numerically tracked with longitudinal positions starting between  $-55 \mu\text{m} \leq z_0 \leq 15 \mu\text{m}$  (see Fig. 4). Their initial momenta  $p_{z,0}$  were randomly distributed, corresponding to an energy range of  $0 \leq \mathcal{E}_0 < 700 \text{ MeV}$ . Starting positions and energies result in the time delay via  $t_D = (z^* - z_0)/(\beta_0 c) - t_{\text{LP}}$ , where  $z_0$  is the starting position,  $\beta_0 c$  is the starting velocity, and  $t_{\text{LP}}$  is the propagation time for the laser maximum to reach the reference plane at  $z^*$ . Transversely, particles were randomly distributed with  $0 \leq r_{\perp,0} \leq 0.25 \mu\text{m}$  and no momentum in these directions.

As long as the particle beam arrives with or after the laser maximum in the focal plane, for a large tolerance of over 200 fs, an energy boost between 30 – 80 MeV is observed. Particles that arrive outside this window are decelerated by less than 15 MeV. In Fig. 2, five possible consecutive stages are marked from 80 to 380 MeV. The inset shows a zoomed detail for stage 1, showing a “flat-

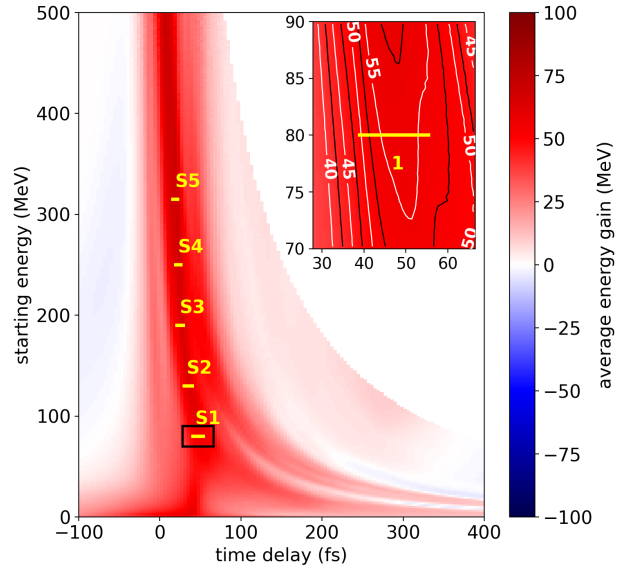


FIG. 2. *Longitudinal beam acceptance.* Average energy gain for tracked beam particles versus their starting energy and arrival time offset with respect to the laser maximum at  $z^* = 15 \mu\text{m}$ . The laser maximum is behind (before) the particle beam for negative (positive) times. Yellow horizontal lines mark design energies for five consecutive stages (S1–5) to boost a beam from 80 MeV to 380 MeV starting energy. The inset zooms into a region around stage S1 (black rectangle) where contour lines mark levels of constant energy gain.

tened” region of uniform acceleration for intense beams of up to 15 fs in length.

Figure 3 shows the correlation of transverse normalized momenta with radial position for beam acceptance into the booster stage. For each stage S1 – S5 in Fig. 2, a proton beam is tracked including transverse momentum variations. Particle tracking per beam covered longitudinal beam positions of  $2 \mu\text{m}$  and transverse initial positions within a disk of  $0 \leq r_{\perp,0} = (x_0^2 + y_0^2)^{1/2} \leq 2 \mu\text{m}$ . Due to the cylindrical symmetry of the channel, a cylindrical symmetry of energy gaining regions in  $x$ - $y$  and  $p_x$ - $p_y$  seems natural. To test this, particles were selected from initial phase space regions  $0 \leq x \leq 0.25 \mu\text{m}$ , and  $0 \leq \theta = \arcsin |p_x/p_z|$ . The angle  $\theta$  is chosen such that particles can only deviate in  $x$  by  $\pm 0.25 \mu\text{m}$  between starting point and channel entrance. The upper row (a) of Fig. 3 thus represents an initial  $y$ - $p_y$  variation. Lower row (b) limits  $y$  and  $p_y$  in the same manner and represents  $x$ - $p_x$  variation for the beam particles. The normalized transverse momentum  $p_{\perp}/p_z$  is shown versus radial distance  $r_{\perp}$ , where  $p_{\perp} = (p_x^2 + p_y^2)^{1/2}$ . Color-coded is the longitudinal energy gain (only corresponding to  $\Delta p_z$ ) between 0 and 90 MeV. Spaced at every 10 MeV we show contour lines of constant energy gain. Phase space regions leading to high energy boost consistently extend from positive transverse momentum at zero ra-

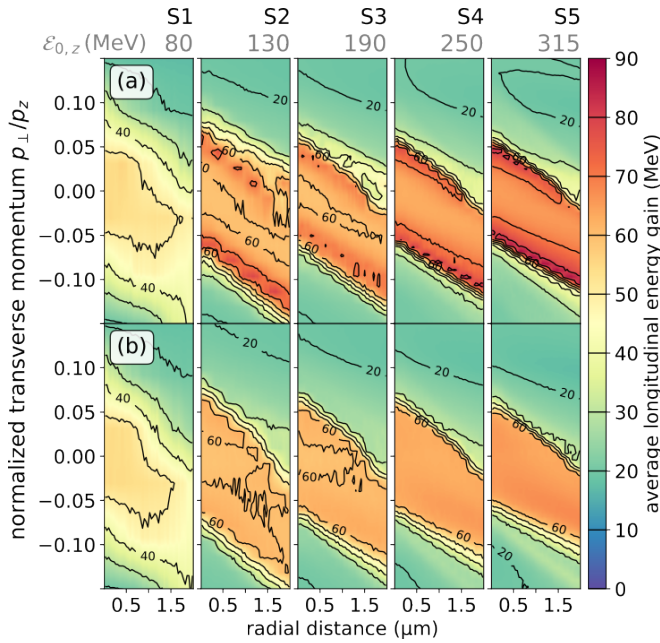


FIG. 3. *Transverse beam acceptance.* Average energy gain corresponding to  $\Delta p_z$  of tracked particles with respect to initial radial distance  $r_\perp$  and initial normalized transverse momentum  $p_\perp/p_{z,0}$ . Row (a) represents a narrow selection around  $x = 0$  and  $p_x = 0$ , resulting in variation mostly in the  $y - p_y$  phase space plane. Row (b) respectively represents varying starting conditions in the  $x - p_x$  plane. The drive laser pulse is  $x$ -polarized.

dial distance to negative normalized transverse momenta at higher distances.

Slightly diverging beams on axis are still accepted by the stage. With growing radial distance only focused, converging beams (negative normalized transverse momentum) are still accepted. The laser in all simulations is  $x$ -polarized. Beams distributed normal to the laser polarization, in  $y - p_y$  as seen in Fig. 3 (a), lead to higher boosts than beams varying in  $x - p_x$ . Remarkably, for beams with initial energies larger than 130 MeV, particles on the beam axis and without transverse momentum do not experience the highest gain. They only gain between 60–70 MeV. Instead, low initial transverse momenta outside the polarization plane allow for boosts up to 80–90 MeV, which is favorable for slight emittance increase over stages.

Based on Eq. 2, we can estimate that the transverse acceptance corresponds to  $R_{\text{ch}}$ , the laser-widened channel radius. The maximum accepted beam emittance can be approximated from the panels in Fig. 3. As an example, consider the  $y - p_y$  phase space in stage S5 (upper panel). Particles in the red-orange region experience an energy gain beyond 50 MeV, and the phase space area of this region is  $0.2 \mu\text{m} \cdot \text{rad}$ . For a beam with a Kapchinskij-Vladimirskij (KV) distribution [61], one can estimate the maximum accepted emittance by dividing this area by  $2\pi$  (instead of  $4\pi$ , due to projection of phase space to

radial distance instead of transverse position) and multiplying by  $\beta\gamma(315 \text{ MeV})$  results in a normalized emittance of  $e_y \leq 28 \text{ nm}$  for a beam in stage S5. For lower energy stages such as S1 and S2, the approximate accepted normalized emittance is only  $\leq 7 \text{ nm}$  and  $\leq 20 \text{ nm}$ , respectively. This suggests that the herein proposed scheme increases in charge-transport efficiency for higher initial beam energies and later stages.

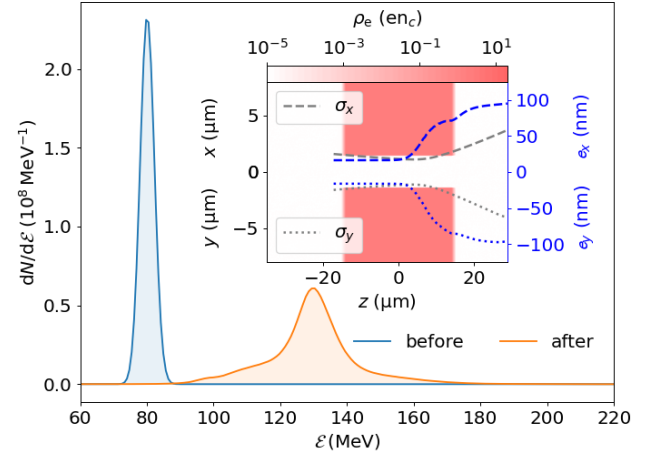


FIG. 4. Energy spectrum of a 200 pC proton beam before (blue) and after (orange) the MVA booster element. The inset shows the initial electron density distribution (red shaded area) of the stage in the  $x - z$  and  $y - z$  half-planes. Furthermore, grey lines show the evolution of transverse RMS beam sizes  $\sigma_x$  (dashed) and  $\sigma_y$  (dotted, mirrored downwards) along the longitudinal coordinate. Blue lines show the evolution of normalized transverse emittance  $e_x$  (dashed) and  $e_y$  (dotted), respectively.

In Figure 4, the scheme is demonstrated by modeling the energy boost of an intense proton beam, with significant charge (200 pC) and space-charge effects, as readily available from Petawatt laser-plasma interaction. Based on the expectations set by the results shown above, this space-charge dominated beam was configured to match the regions of longitudinal and transverse acceptance in Figs. 2 and 3. No further optimization of the scheme has been performed and future design optimizations to beam-, laser pulse- and booster stage density-profile can be explored.

In practice, the 200 pC of charge are energy-selected and ideally transported via, e.g., a suitable solenoid-beamline [62]. It is assumed that the beam has been phase-space rotated in a similar fashion as described by Busold *et al.* [63]. In this simulation, the incoming beam has a relative momentum spread of  $\sigma_{p_z}/\langle p_z \rangle = 1.37\%$ . It is focused towards the region and time of strongest accelerating field, at  $z^* = 15 \mu\text{m}$  and coincides with the maximum laser field at the stage rear. The beam's initial, normalized emittance is  $e_x = e_y = 16.25 \text{ nm}$ , a value simulated from a laser-plasma proton source in [31]. The beam is initialized at  $\langle z \rangle_0 = -17.3 \mu\text{m}$  such that in vac-

uum and without considering space charge it would drift towards its focus with Courant-Snyder (Twiss) parameters of  $\beta_{x,f} = \beta_{y,f} = 25.9 \mu\text{m}$ ,  $\alpha_{x,f} = \alpha_{y,f} = 0$ , and  $\gamma_{x,f} = \gamma_{y,f} = 38\,553 \text{ m}^{-1}$ .

The central energy of the beam is boosted in the stage by 50 MeV, as predicted by Fig. 2. No beam charge is lost during the acceleration process. In the inset, we show the emittance and beam envelope evolution. After the first booster stage, the emittance has grown to just below 100 nm in both transverse directions (see inset). The longitudinal momentum spread grew to just over 5%. In the simulation, it is observable that this growth originates from strong transient electric fields created by the laser pulse-wall interaction as it overtakes the beam towards the exit of the channel.

In summary, we present a novel scheme for boosting the energy of intense ion beams to from available non-relativistic sources to the relativistic regime, confirmed by 3D simulations. A hollow target is used in combination with the magnetic vortex acceleration mechanism to act as a booster stage, benefitting from its combined acceleration and focusing properties at the 10s of MV/*mum* scale. We showed that a space-charge dominated proton beam from an laser-proton source, as is readily available at Petawatt laser facilities, can be boosted to high  $\beta$  without the loss of charge. We demonstrated that our scheme is scalable to arbitrary  $\beta$ . As such, our scheme is applicable as a booster to laser-driven ion sources and their readily attainable 60-100 MeV beams. The required matching depends on the spatial beam focus and time delay between the drive laser pulse and the arrival of the beam. The mechanism is robust, featuring good acceptance and high potential for design optimizations.

The authors would like to thank Ryan T. Sandberg and Davide Terzani for helpful discussions. Simulations used the open source particle-in-cell code WarpX in version

23.01. Simulation inputs, analysis scripts, source code and data are available in Refs. [59, 64]. We acknowledge all WarpX contributors. Primary WarpX contributors are with LBNL, LLNL, CEA-LIDYL, SLAC, DESY, CERN, and TAE. This material is based upon work supported by the Defense Advanced Research Projects Agency via Northrop Grumman Corporation. S. Hakimi was supported by the U.S. DOE FES Postdoctoral Research Program administered by the OAK Ridge Institute for Science and Education (ORISE) for the DOE. ORISE is managed by Oak Ridge Associated Universities (ORAU) under DOE contract number DE-SC0014664. All opinions expressed in this paper are the author's and do not necessarily reflect the policies and views of DOE, ORAU, or ORISE. This research was supported by the U.S. DOE Office of Science Offices of HEP and FES (through LaserNetUS) under Contract No. DE-AC02-05CH11231 and the Exascale Computing Project (17-SC-20-SC), a collaborative effort of the U.S. Department of Energy Office of Science and the National Nuclear Security Administration. This research was supported by the U.S. Department of Energy, Office of Science, Office of Advanced Scientific Computing Research and Office of High Energy Physics, Scientific Discovery through Advanced Computing (SciDAC) program. An award of computer time was provided by the ASCR Leadership Computing Challenge (ALCC) program. This research used resources of the Oak Ridge Leadership Computing Facility at the Oak Ridge National Laboratory, which is supported by the Office of Science of the U.S. Department of Energy under Contract No. DE-AC05-00OR22725. This research used resources of the National Energy Research Scientific Computing Center (NERSC), a U.S. Department of Energy Office of Science User Facility located at Lawrence Berkeley National Laboratory, operated under Contract No. DE-AC02-05CH11231 using NERSC award FES-ERCAP0024250.

- 
- [1] C. Geddes, M. Hogan, P. Musumeci, and R. Assmann, Report of snowmass 21 accelerator frontier topical group 6 on advanced accelerators (2022).
- [2] C. N. Danson, C. Haefner, J. Bromage, T. Butcher, J.-C. F. Chanteloup, E. A. Chowdhury, A. Galvanauskas, L. A. Gizzi, J. Hein, D. I. Hillier, *et al.*, Petawatt and exawatt class lasers worldwide, *High Power Laser Science and Engineering* **7** (2019).
- [3] A. Gonoskov, T. G. Blackburn, M. Marklund, and S. S. Bulanov, Charged particle motion and radiation in strong electromagnetic fields, *Rev. Mod. Phys.* **94**, 045001 (2022).
- [4] J. W. Yoon, Y. G. Kim, I. Choi, J. H. Sung, H. W. Lee, S. K. Lee, and C. H. Nam, Realization of laser intensity over  $10^{23} \text{ W/cm}^2$ , *Optica* **8**, 630 (2021).
- [5] G. A. Mourou, T. Tajima, and S. V. Bulanov, Optics in the relativistic regime, *Rev. Mod. Phys.* **78**, 309 (2006).
- [6] H. Daido, M. Nishiuchi, and A. S. Pirozhkov, Review of laser-driven ion sources and their applications, *Reports on Progress in Physics* **75**, 056401 (2012).
- [7] A. Macchi, M. Borghesi, and M. Passoni, Ion acceleration by superintense laser-plasma interaction, *Reviews of Modern Physics* **85**, 751 (2013).
- [8] S. S. Bulanov, E. Esarey, C. B. Schroeder, S. V. Bulanov, T. Z. Esirkepov, M. Kando, F. Pegoraro, and W. P. Lee-mans, Radiation pressure acceleration: The factors limiting maximum attainable ion energy, *Physics of Plasmas* **23**, 056703 (2016).
- [9] M. Rehwald, S. Assenbaum, C. Bernert, F.-E. Brack, M. Bussmann, T. E. Cowan, C. B. Curry, F. Fiuza, M. Garten, L. Gaus, M. Gauthier, S. Göde, I. Göthel, S. H. Glenzer, L. Huang, A. Huebl, J. B. Kim, T. Kluge, S. Kraft, F. Kroll, J. Metzkes-Ng, T. Miethlinger, M. Loeser, L. Obst-Huebl, M. Reimold, H.-P. Schlenvoigt, C. Schoenwaelder, U. Schramm, M. Siebold, F. Tr-effert, L. Yang, T. Ziegler, and K. Zeil, Ultra-short pulse laser acceleration of protons to 80 mev from cryogenic hydrogen jets tailored to near-critical density, *Nature Com-*

- munications **14**, 4009 (2023).
- [10] F. Wagner, O. Deppert, C. Brabetz, P. Fiala, A. Klein-schmidt, P. Poth, V. A. Schanz, A. Tebartz, B. Zielbauer, M. Roth, T. Stöhlker, and V. Bagnoud, Maximum proton energy above 85 mev from the relativistic interaction of laser pulses with micrometer thick  $\text{ch}_2$  targets, *Phys. Rev. Lett.* **116**, 205002 (2016).
- [11] A. Higginson, R. J. Gray, M. King, R. J. Dance, S. D. R. Williamson, N. M. H. Butler, R. Wilson, R. Capdessus, C. Armstrong, J. S. Green, S. J. Hawkes, P. Martin, W. Q. Wei, S. R. Mirfayzi, X. H. Yuan, S. Kar, M. Borghesi, R. J. Clarke, D. Neely, and P. McKenna, Near-100 MeV protons via a laser-driven transparency-enhanced hybrid acceleration scheme, *Nature Communications* **9**, 10.1038/s41467-018-03063-9 (2018).
- [12] N. P. Dover, T. Ziegler, S. Assenbaum, C. Bernert, S. Bock, F.-E. Brack, T. E. Cowan, E. J. Ditter, M. Garten, L. Gaus, I. Goethel, G. S. Hicks, H. Kiriyama, T. Kluge, J. K. Koga, A. Kon, K. Kondo, S. Kraft, F. Kroll, H. F. Lowe, J. Metzkes-Ng, T. Miyatake, Z. Najmudin, T. Püschel, M. Rehwald, M. Reimold, H. Sakaki, H.-P. Schlenvoigt, K. Shiokawa, M. E. P. Umlandt, U. Schramm, K. Zeil, and M. Nishiuchi, Enhanced ion acceleration from transparency-driven foils demonstrated at two ultraintense laser facilities, *Light: Science & Applications* **12**, 71 (2023).
- [13] S. V. Bulanov and V. S. Khoroshkov, Feasibility of using laser ion accelerators in proton therapy, *Plasma Physics Reports* **28**, 453 (2002).
- [14] S. V. Bulanov, J. J. Wilkens, T. Z. Esirkepov, G. Korn, G. Kraft, S. D. Kraft, M. Molls, and V. S. Khoroshkov, Laser ion acceleration for hadron therapy, *Physics-Uspekhi* **57**, 1149 (2014).
- [15] L. Karsch, E. Beyreuther, W. Enghardt, M. Gotz, U. Masood, U. Schramm, K. Zeil, and J. Pawelke, Towards ion beam therapy based on laser plasma accelerators, *Acta Oncologica* **56**, 1359 (2017), pMID: 28828925, <https://doi.org/10.1080/0284186X.2017.1355111>.
- [16] B. Shen, Y. Li, M. Y. Yu, and J. Cary, Bubble regime for ion acceleration in a laser-driven plasma, *Phys. Rev. E* **76**, 055402 (2007).
- [17] E. Esarey, C. B. Schroeder, and W. P. Leemans, Physics of laser-driven plasma-based electron accelerators, *Rev. Mod. Phys.* **81**, 1229 (2009).
- [18] M. Liu, S. M. Weng, H. C. Wang, M. Chen, Q. Zhao, Z. M. Sheng, M. Q. He, Y. T. Li, and J. Zhang, Efficient injection of radiation-pressure-accelerated sub-relativistic protons into laser wakefield acceleration based on 10 PW lasers, *Physics of Plasmas* **25**, 063103 (2018).
- [19] S. Steinke, J. van Tilborg, C. Benedetti, C. G. R. Geddes, C. B. Schroeder, J. Daniels, K. K. Swanson, A. J. Gonsalves, K. Nakamura, N. H. Matlis, B. H. Shaw, E. Esarey, and W. P. Leemans, Multistage coupling of independent laser-plasma accelerators, *Nature* **530**, 190 (2016).
- [20] A. V. Kuznetsov, T. Z. Esirkepov, F. F. Kamenets, and S. V. Bulanov, Efficiency of ion acceleration by a relativistically strong laser pulse in an underdense plasma, *Plasma Physics Reports* **27**, 211 (2001).
- [21] S. V. Bulanov, Ion acceleration in a dipole vortex in a laser plasma corona, *Plasma Physics Reports* **31**, 369 (2005).
- [22] S. V. Bulanov and T. Z. Esirkepov, Comment on “collimated multi-mev ion beams from high-intensity laser interactions with underdense plasma”, *Physical Review Letters* **98**, 049503 (2007).
- [23] S. S. Bulanov, V. Y. Bychenkov, V. Chvykov, G. Kalinchenko, D. W. Litzenberg, T. Matsuoka, A. G. R. Thomas, L. Willingale, V. Yanovsky, K. Krushelnick, and A. Maksimchuk, Generation of gev protons from 1 pw laser interaction with near critical density targets, *Physics of Plasmas* **17**, 043105 (2010).
- [24] J. Park, S. S. Bulanov, J. Bin, Q. Ji, S. Steinke, J.-L. Vay, C. G. R. Geddes, C. B. Schroeder, W. P. Leemans, T. Schenkel, and E. Esarey, Ion acceleration in laser generated megatesla magnetic vortex, *Physics of Plasmas* **26**, 103108 (2019).
- [25] K. Matsukado, T. Esirkepov, K. Kinoshita, H. Daido, T. Utsumi, Z. Li, A. Fukumi, Y. Hayashi, S. Orimo, M. Nishiuchi, S. V. Bulanov, T. Tajima, A. Noda, Y. Iwashita, T. Shirai, T. Takeuchi, S. Nakamura, A. Yamazaki, M. Ikegami, T. Mihara, A. Morita, M. Uesaka, K. Yoshii, T. Watanabe, T. Hosokai, A. Zhidkov, A. Ogata, Y. Wada, and T. Kubota, Energetic protons from a few-micron metallic foil evaporated by an intense laser pulse, *Physical Review Letters* **91**, 215001 (2003).
- [26] L. Willingale, S. P. D. Mangles, P. M. Nilson, R. J. Clarke, A. E. Dangor, M. C. Kaluza, S. Karsch, K. L. Lancaster, W. B. Mori, Z. Najmudin, J. Schreiber, A. G. R. Thomas, M. S. Wei, and K. Krushelnick, Collimated multi-mev ion beams from high-intensity laser interactions with underdense plasma, *Phys. Rev. Lett.* **96**, 245002 (2006).
- [27] A. Yogo, H. Daido, S. V. Bulanov, K. Nemoto, Y. Oishi, T. Nayuki, T. Fujii, K. Ogura, S. Orimo, A. Sagisaka, J.-L. Ma, T. Z. Esirkepov, M. Mori, M. Nishiuchi, A. S. Pirozhkov, S. Nakamura, A. Noda, H. Nagatomo, T. Kimura, and T. Tajima, Laser ion acceleration via control of the near-critical density target, *Physical Review E* **77**, 016401 (2008).
- [28] Y. Fukuda, A. Y. Faenov, M. Tampo, T. A. Pikuz, T. Nakamura, M. Kando, Y. Hayashi, A. Yogo, H. Sakaki, T. Kameshima, A. S. Pirozhkov, K. Ogura, M. Mori, T. Z. Esirkepov, J. Koga, A. S. Boldarev, V. A. Gasilov, A. I. Magunov, T. Yamauchi, R. Kodama, P. R. Bolton, Y. Kato, T. Tajima, H. Daido, and S. V. Bulanov, Energy increase in multi-mev ion acceleration in the interaction of a short pulse laser with a cluster-gas target, *Phys. Rev. Lett.* **103**, 165002 (2009).
- [29] L. Willingale, S. R. Nagel, A. G. R. Thomas, C. Bellei, R. J. Clarke, A. E. Dangor, R. Heathcote, M. C. Kaluza, C. Kamperidis, S. Kneip, K. Krushelnick, N. Lopes, S. P. D. Mangles, W. Nazarov, P. M. Nilson, and Z. Najmudin, Characterization of high-intensity laser propagation in the relativistic transparent regime through measurements of energetic proton beams, *Physical Review Letters* **102**, 125002 (2009).
- [30] L. Willingale, P. M. Nilson, A. G. R. Thomas, S. S. Bulanov, A. Maksimchuk, W. Nazarov, T. C. Sangster, C. Stoeckl, and K. Krushelnick, High-power, kilojoule laser interactions with near-critical density plasma, *Physics of Plasmas* **18**, 056706 (2011).
- [31] S. Hakimi, L. Obst-Huebl, A. Huebl, K. Nakamura, S. S. Bulanov, S. Steinke, W. P. Leemans, Z. Kober, T. M. Ostermayr, T. Schenkel, A. J. Gonsalves, J.-L. Vay, J. van Tilborg, C. Toth, C. B. Schroeder, E. Esarey, and C. G. R. Geddes, Laser-solid interaction studies enabled by the new capabilities of the ip2 bella pw beamline,

- Physics of Plasmas **29**, 083102 (2022).
- [32] O. Jäckel, S. M. Pfotenhauer, J. Polz, S. Steinke, H. P. Schlenvoigt, J. Heymann, A. P. L. Robinson, and M. C. Kaluza, Staged laser ion acceleration (OSA, 2009) p. JFB1.
- [33] W. P. Wang, B. F. Shen, X. M. Zhang, X. F. Wang, J. C. Xu, X. Y. Zhao, Y. H. Yu, L. Q. Yi, Y. Shi, L. G. Zhang, T. J. Xu, and Z. Z. Xu, Cascaded target normal sheath acceleration, *Physics of Plasmas* **20**, 10.1063/1.4831943 (2013).
- [34] S. Kawata, D. Sato, T. Izumiyama, T. Nagashima, M. Takano, D. Barada, Y. Y. Ma, W. M. Wang, Q. Kong, P. X. Wang, and Y. J. Gu, Multi-stage ion acceleration in laser plasma interaction (Journal of the Physical Society of Japan, 2014).
- [35] S. M. Pfotenhauer, O. Jäckel, J. Polz, S. Steinke, H.-P. Schlenvoigt, J. Heymann, A. P. L. Robinson, and M. C. Kaluza, A cascaded laser acceleration scheme for the generation of spectrally controlled proton beams, *New Journal of Physics* **12**, 103009 (2010).
- [36] T. E. Cowan, J. Fuchs, H. Ruhl, A. Kemp, P. Audebert, M. Roth, R. Stephens, I. Barton, A. Blazevic, E. Brambrink, J. Cobble, J. Fernández, J.-C. Gauthier, M. Geissel, M. Hegelich, J. Kaae, S. Karsch, G. P. L. Sage, S. Letzring, M. Mancossi, S. Meyroneinc, A. Newkirk, H. Pépin, and N. Renard-LeGalloudec, Ultralow emittance, multi-mev proton beams from a laser virtual-cathode plasma accelerator, *Physical Review Letters* **92**, 204801 (2004).
- [37] M. Borghesi, A. J. Mackinnon, D. H. Campbell, D. G. Hicks, S. Kar, P. K. Patel, D. Price, L. Romagnani, A. Schiavi, and O. Willi, Multi-mev proton source investigations in ultraintense laser-foil interactions, *Physical Review Letters* **92**, 055003 (2004).
- [38] F. Nürnberg, M. Schollmeier, E. Brambrink, A. Blažević, D. C. Carroll, K. Flippo, D. C. Gautier, M. Geißel, K. Harres, B. M. Hegelich, O. Lundh, K. Markey, P. McKenna, D. Neely, J. Schreiber, and M. Roth, Radiochromic film imaging spectroscopy of laser-accelerated proton beams, *Review of Scientific Instruments* **80**, 10.1063/1.3086424 (2009).
- [39] X. Zhang, B. Shen, X. Li, Z. Jin, and F. Wang, Multi-staged acceleration of ions by circularly polarized laser pulse: Monoenergetic ion beam generation, *Physics of Plasmas* **14**, 073101 (2007).
- [40] T. Toncian, M. Borghesi, J. Fuchs, E. d’Humieres, P. Antici, P. Audebert, E. Brambrink, C. A. Cecchetti, A. Pipahl, L. Romagnani, and O. Willi, Ultrafast laser-driven microlens to focus and energy-select mega-electron volt protons, *Science* **312**, 410 (2006).
- [41] S. Kar, H. Ahmed, R. Prasad, M. Cerchez, S. Brauckmann, B. Aurand, G. Cantono, P. Hadjisolomou, C. L. S. Lewis, A. Macchi, G. Nersisyan, A. P. L. Robinson, A. M. Schroer, M. Swantusch, M. Zepf, O. Willi, and M. Borghesi, Guided post-acceleration of laser-driven ions by a miniature modular structure, *Nature Communications* **7**, 10792 (2016).
- [42] S. Ferguson, P. Martin, H. Ahmed, E. Aktan, M. Alanazi, M. Cerchez, D. Doria, J. S. Green, B. Greenwood, B. Odlozilik, O. Willi, M. Borghesi, and S. Kar, Dual stage approach to laser-driven helical coil proton acceleration, *New Journal of Physics* **25**, 013006 (2023).
- [43] V. Y. Bychenkov and G. I. Dudnikova, Two-stage laser acceleration of ions, *Plasma Physics Reports* **33**, 655 (2007).
- [44] A. Yogo, K. Mima, N. Iwata, S. Tosaki, A. Morace, Y. Arikawa, S. Fujioka, T. Johzaki, Y. Sentoku, H. Nishimura, A. Sagisaka, K. Matsuo, N. Kamitsukasa, S. Kojima, H. Nagatomo, M. Nakai, H. Shiraga, M. Murakami, S. Tokita, J. Kawanaka, N. Miyanaga, K. Yamanoi, T. Norimatsu, H. Sakagami, S. V. Bulanov, K. Kondo, and H. Azechi, Boosting laser-ion acceleration with multi-picosecond pulses, *Scientific Reports* **7**, 42451 (2017).
- [45] J. Kim, S. Wilks, A. Kemp, M. Sherlock, T. Ma, F. Beg, and D. Mariscal, Efficient ion acceleration by multistaged intense short laser pulses, *Physical Review Research* **4**, L032003 (2022).
- [46] H. C. Wang, S. M. Weng, M. Murakami, Z. M. Sheng, M. Chen, Q. Zhao, and J. Zhang, Cascaded acceleration of proton beams in ultrashort laser-irradiated microtubes, *Physics of Plasmas* **24**, 10.1063/1.5000104 (2017).
- [47] A. Ting, B. Hafizi, M. Helle, Y. H. Chen, D. Gordon, D. Kaganovich, M. Polyanskiy, I. Pogorelsky, M. Babzien, C. Miao, N. Dover, Z. Najmudin, and O. Etlinger, Staging and laser acceleration of ions in underdense plasma (American Institute of Physics Inc., 2017).
- [48] J. B. Kim, S. Göde, and S. H. Glenzer, Development of a cryogenic hydrogen microjet for high-intensity, high-repetition rate experiments, *Review of Scientific Instruments* **87**, 11E328 (2016), [https://pubs.aip.org/aip/rsi/article-pdf/doi/10.1063/1.4961089/16054498/11e328\\_1.online.pdf](https://pubs.aip.org/aip/rsi/article-pdf/doi/10.1063/1.4961089/16054498/11e328_1.online.pdf).
- [49] S. Göde, C. Rödel, K. Zeil, R. Mishra, M. Gauthier, F.-E. Brack, T. Kluge, M. J. MacDonald, J. Metzkes, L. Obst, M. Rehwald, C. Ruyer, H.-P. Schlenvoigt, W. Schumaker, P. Sommer, T. E. Cowan, U. Schramm, S. Glenzer, and F. Fiuza, Relativistic electron streaming instabilities modulate proton beams accelerated in laser-plasma interactions, *Phys. Rev. Lett.* **118**, 194801 (2017).
- [50] Z. Gong, S. S. Bulanov, T. Toncian, and A. Arefiev, Energy-chirp compensation of laser-driven ion beams enabled by structured targets, *Phys. Rev. Res.* **4**, L042031 (2022).
- [51] K. V. Lezhnin and S. V. Bulanov, Laser ion acceleration from tailored solid targets with micron-scale channels, *Physical Review Research* **4**, 10.1103/PhysRevResearch.4.033248 (2022).
- [52] X.-L. Zhu, W.-Y. Liu, M. Chen, S.-M. Weng, P. McKenna, Z.-M. Sheng, and J. Zhang, Bunched proton acceleration from a laser-irradiated cone target, *Physical Review Applied* **18**, 044051 (2022).
- [53] I. Tazes, S. Passalidis, E. Kaselouris, I. Fitis, M. Bakarezos, N. A. Papadogiannis, M. Tatarakis, and V. Dimitriou, A computational study on the optical shaping of gas targets via blast wave collisions for magnetic vortex acceleration, *High Power Laser Science and Engineering* **10**, 10.1017/hpl.2022.16 (2022).
- [54] J. Snyder, L. L. Ji, K. M. George, C. Willis, G. E. Cochran, R. L. Daskalova, A. Handler, T. Rubin, P. L. Poole, D. Nasir, A. Zingale, E. Chowdhury, B. F. Shen, and D. W. Schumacher, Relativistic laser driven electron accelerator using micro-channel plasma targets, *Physics of Plasmas* **26**, 033110 (2019).
- [55] M. Bailly-Grandvaux, D. Kawahito, C. McGuffey, J. Strehlow, B. Edghill, M. S. Wei, N. Alexander, A. Haid, C. Brabetz, V. Bagnoud, R. Hollinger, M. G. Capeluto, J. J. Rocca, and F. N. Beg, Ion acceleration

- from microstructured targets irradiated by high-intensity picosecond laser pulses, *Phys. Rev. E* **102**, 021201 (2020).
- [56] H. Rinderknecht, T. Wang, A. L. Garcia, G. Bruhaug, M. Wei, H. Quevedo, T. Ditmire, J. Williams, A. Haid, D. Doria, *et al.*, Relativistically transparent magnetic filaments: scaling laws, initial results and prospects for strong-field qed studies, *New Journal of Physics* **23**, 095009 (2021).
- [57] S. S. Bulanov, E. Esarey, C. B. Schroeder, W. P. Lee-mans, S. V. Bulanov, D. Margarone, G. Korn, and T. Haberer, Helium-3 and helium-4 acceleration by high power laser pulses for hadron therapy, *Phys. Rev. ST Accel. Beams* **18**, 061302 (2015).
- [58] L. Fedeli, A. Huebl, F. Boillod-Cerneux, T. Clark, K. Gott, C. Hillairet, S. Jaure, A. Leblanc, R. Lehe, A. Myers, C. Piechurski, M. Sato, N. Zaim, W. Zhang, J.-L. Vay, and H. Vincenti, Pushing the Frontier in the Design of Laser-Based Electron Accelerators with Ground-breaking Mesh-Refined Particle-In-Cell Simulations on Exascale-Class Supercomputers, in *SC22: International Conference for High Performance Computing, Networking, Storage and Analysis* (2022) pp. 1–12.
- [59] J.-L. Vay, A. Almgren, L. D. Amorim, I. Andriyash, D. Belkin, D. Bizzozero, A. Blelly, S. E. Clark, L. Fedeli, M. Garten, L. Ge, K. Gott, C. Harrison, A. Huebl, L. Giacomel, R. E. Groenewald, D. Grote, J. Gu, R. Jambunathan, H. Klion, P. Kumar, M. Thevenet, G. Richardson, O. Shapoval, R. Lehe, B. Loring, P. Miller, A. Myers, E. Rheaume, M. E. Rowan, R. T. Sandberg, P. Scherpelz, E. Yang, W. Zhang, Y. Zhao, K. Z. Zhu, E. Zoni, and N. Zaim, *WarpX* (2018), <https://ecp-warpX.github.io> <https://doi.org/10.5281/zenodo.4571577>.
- [60] L. Obst-Huebl, K. Nakamura, S. Hakimi, J. T. D. Chant, A. Jewell, B. Stassel, A. M. Snijders, A. J. Gon-salves, J. van Tilborg, Z. Eisentraut, Z. Harvey, L. Will-ingale, C. Toth, C. B. Schroeder, C. G. R. Geddes, and E. Esarey, High power commissioning of BELLA iP2 up to 17 J, in *Applying Laser-driven Particle Acceleration III: Using Distinctive Energetic Particle and Photon Sources*, Vol. 12583, edited by J. Schreiber and P. R. Bolton, International Society for Optics and Photonics (SPIE, 2023) p. 1258305.
- [61] I. Kapchinskij and V. Vladimirkij, Limitations of proton beam current in a strong focusing linear accelerator associated with the beam space charge, in *Proceedings of the International Conference on High Energy Accelerators and Instrumentation* (CERN Scientific Information Service Geneva, 1959) p. 274.
- [62] F.-E. Brack, F. Kroll, L. Gaus, C. Bernert, E. Beyreuther, T. E. Cowan, L. Karsch, S. Kraft, L. A. Kunz-Schughart, E. Lessmann, J. Metzkes-Ng, L. Obst-Huebl, J. Pawelke, M. Rehwald, H.-P. Schlen-voigt, U. Schramm, M. Sobiella, E. R. Szabó, T. Ziegler, and K. Zeil, Spectral and spatial shaping of laser-driven proton beams using a pulsed high-field magnet beamline, *Scientific Reports* **10**, 9118 (2020).
- [63] S. Busold, D. Schumacher, C. Brabetz, O. Deppert, F. Kroll, A. Blazevic, V. Bagnoud, and M. Roth, The light beamline at gsi: Shaping intense mev proton bunches from a compact laser-driven source, *IPAC 2014 10.18429/JACoW-IPAC2014-TUPME030* (2014).
- [64] M. Garten, S. S. Bulanov, S. Hakimi, C. E. Obst-Huebl, Lieselotte Mitchell, C. Schroeder, E. Esarey, C. G. R. Geddes, J.-L. Vay, and A. Huebl, *Data Archive*, 10.5281/zenodo.8210206 (2023).